Hindawi
Geofluids
Volume 2019, Article ID 5387907, 12 pages
https://doi.org/10.1155/2019/5387907

Research Article

Crack Initiation Characteristics of Gas-Containing Coal under Gas Pressures

Zhiqiang Yin[1,2] **Zhiyu Chen**[1] **Jucai Chang**[1] **Zuxiang Hu**[1] **Haifeng Ma**[1] **and Ruimin Feng**[3]

[1]*Key Laboratory of Safe and Effective Coal Mining, Anhui University of Science and Technology, Huainan, 232001 Anhui, China*
[2]*School of Civil and Mechanical Engineering, Curtin University, Perth, 6102 Western Australia, Australia*
[3]*Department of Chemical and Petroleum Engineering, University of Calgary, Calgary, Canada T2N 1N4*

Correspondence should be addressed to Zhiqiang Yin; zhqyin@aust.edu.cn

Received 23 June 2018; Revised 29 August 2018; Accepted 19 November 2018; Published 7 February 2019

Guest Editor: Wen Wang

In deep coal mines, coal before the working face is subjected to coupled high mining-induced stress and gas pressure. Such condition may facilitate crack formation and propagation in the coal seam, leading to serious coal and gas disasters. In this study, the mechanical properties (i.e., uniaxial compressive strength, tensile strength, and fracture toughness) of gas-containing coal with four levels of initial gas pressure (i.e., 0.0, 0.5, 1.0, and 1.5 MPa) were investigated by uniaxial compression, Brazilian disc, and notched semicircular bending loading test. A newly developed gas-sealing device and an RMT-150 rock mechanics testing machine were used. Fracture modes under different initial gas pressures were also determined. A theoretical method of fracture mechanics was used to analyze crack initiation characteristics under gas adsorption state. Results show that the uniaxial compressive strength, tensile strength, and fracture toughness of gas-containing coal decreased with increasing initial gas pressure. The tensional fracture occurred in gas-containing coal under uniaxial compressive loading with high gas pressure. Cracks in gas-containing coal propagated under small external loads due to the increase in effective stress of crack tip and decrease in cracking strength. This study provided evidence for modifications of the support design of working face in deep coal mines. Furthermore, the correlations between fracture toughness, compressive strength, and tensile strength of gas-containing coal were investigated.

1. Introduction

With the increase in the mining depth of coal mines in eastern China, the geological and mechanical environments of deep mines differ from those of shallow mines. The most typical change is that the proportion of high-gas-pressure coal seam increases (most gases are methane) and gravity stress and mining-induced stress also increase obviously. A large number of in situ investigations and numerical simulations have demonstrated that the primary cracks in coal seam before the working face will grow and generate new cracks under high mining-induced stress, and the state of adsorbed gas in the coal seam will also change; the direct consequence is that the working face is prone to coal and gas outburst accidents [1–3]. Such dynamic accidents are strong and sudden, which can be destructive and seriously threaten the production of coal mines. The incident mechanism is complicated by coupled high gas pressure and mining-induced stress [4, 5]. Previous studies on the dynamic disasters of coal and gas outbursts in shallow coal seams have indicated that the dynamic disasters of coal and gas outbursts are mainly caused by the expansion of high gas pressure in the coal seams. Theoretical models (i.e., instability and energy models) are established on the basis of the traditional analysis of disaster mechanism on shallow seams [6, 7]. However, the influence of external load on coal and gas outbursts is not accounted in these theoretical models. Consequently, the mechanism of dynamic disasters of coal and gas outbursts in deep coal mines is interpreted inaccurately. In deep mining, the mining-induced stress is obvious on high-gas

coal seams. Therefore, the effect of coupled gas pressure and external load on the dynamic disasters in deep coal mines must be comprehensively considered. The mechanical properties of coal seams under the gas state have become popular topics in coal mining.

The mechanical and adsorption properties of coals have been experimentally and theoretically investigated over the last two decades. On the one hand, considerable gas-sealing equipment has been developed, and experimental studies on the compression loading properties of gas-containing coal have been conducted [8–11]. The strength and damage of gas-containing coal were studied using a coupled gas-solid experimental device by Xie et al. [12]. Their results showed that a high initial gas pressure could decrease sample strength and increase damage degree. The acoustic emission characteristics of gas-containing coal were studied using acoustic emission equipment, and experimental results showed that acoustic emission energy decreased in the process of crack splitting due to the occurrence of gas that significantly influenced crack propagation [13, 14]. The macroscopic crack propagation [15] and fracture toughness [16] of gas-containing coal were tested with increasing initial gas pressure and crack velocity and decreasing fracture toughness. These studies mainly focused on the macroscopic mechanical properties of raw gas-containing coal sample, and results showed that the mechanical properties of coal were obviously weakened by the state of adsorbed gas. On the other hand, coal pore morphology and permeability have been experimentally and theoretically investigated [17–19]. When external stress and temperature conditions change, the effective stress and temperature and the degree of gas desorption increase [20]. During gas production and injection, the morphological evolution of coal pores is a combined effect of effective stress and sorption-induced matrix swelling/shrinkage [21]. During gas extraction, the effective stress increases, which causes cleat closure [22]. Meanwhile, desorption of gas adsorbed on the inner coal surface results in matrix shrinkage, thereby widening cleat aperture. As a result, the overall morphological evolution of coal pores is determined by the balance between these two effects. Most experimental studies focusing on the adsorption characteristics of gas have been conducted at adsorption expansion stress and deformation in coal. The gas pressure in pore or crack is small compared with the adsorption expansion stress. However, in the study of crack initiation characteristics, the gas pressure in the pore or crack is not negligible. Detailed studies of crack initiation and state of adsorbed gas under external stress conditions are limited. Coal is a typical sedimentary rock with multipore medium. Various initial microcracks inevitably exist in coal. The process of coal failure is essentially the process of the initiation, expansion, bifurcation, and perforation of initial microcracks under external loads. Crack propagation and failure in gas-containing coal are closely related to external loads and gas occurrence due to the high gas pressure in deep coal seams. Therefore, the mechanics and failure characteristics of gas-containing coal are necessary to study on the basis of crack initiation characteristics.

In this study, a laboratory investigation of the mechanical properties of raw coal samples under different gas pressures is conducted. The scenarios of increasing mining-induced stress and gas pressure in coal seam before the working face are simulated on the basis of the analysis of field mining-induced stress and gas pressure. The mechanical parameters of gas-containing coal, such as uniaxial compressive strength (σ_{uc}), tensile strength (σ_t), and fracture toughness (K_{IC}), under different initial gas pressures are tested by uniaxial compression (UC), Brazilian disc (BD), and notched semicircular bending (NSCB) loading test, respectively. The correlation among the mechanical parameters is analyzed. The weakening law of gas pressure on mechanical properties is analyzed by a gas-containing crack initiation model, in which the model is based on fracture mechanics and gas adsorption characteristics. The research results have important practical significance and application value to the stability analysis of working face in deep coal seams with high gas pressure.

2. Experimental Procedures

2.1. Specimen Preparation. The coal specimens used in this study are prepared from the Xieqiao Coal Mine in the Huainan mine area of China. The working face of coal seam, which is a typical low-permeability and high-gas-pressure coal seam, is approximately 780 m underground. Microscopic studies are performed to give insights into pore structures and sizes using computed tomography (v tome x L300), as shown in Figure 1. Many small pore structures exist in the coals. The initial permeability of the coal specimens is approximately 0.031 md, the porosity is approximately 4.32%, and the average dry density is 1.395 kg/m^3. The adsorption constants of the coals are 35.428 m^3/t and 1.163 MPa^{-1} at room temperature (26°C).

2.2. Experimental Setup. A novel experimental system is constructed, in which the gas-containing coal specimens can be tested under static loading, as shown in Figure 2. The experimental system is developed by Anhui University of Science and Technology; it mainly includes an RMT-150 rock mechanics testing machine, a gas-sealing device, and a gas supply device. The gas-sealing device is placed on the loading platform of a rock rigidity tester. The pressure head of the tester is connected to the pressure bar of the gas-sealing device to ensure that the sample is loaded. An observation window composed of glass is arranged on one side of the sealing device, which can be used to install the sample and observe the deformation of the specimen during the loading process. The gas supply device is connected to the gas-sealing device through a gas pipeline. Before static pressure is applied, the sample is placed in the gas-sealing device. The air in the gas-sealing device is then pumped out through an air pump to ensure that the air pressure inside the gas-sealing device is 0.1 bar, and the gas (CH_4 99%) is filled into the gas-sealing device. The gas pressure in the gas-sealing device is compensated with a gas cylinder to ensure that the gas pressure is constant, if the change in the gas pressure is more than 1.5% during the processes of static loading test. Two inline holes are drilled in the gas-sealing device and connect the data acquisition device with the wire line.

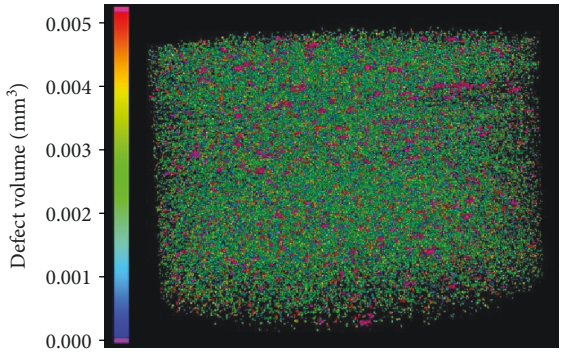

Figure 1: Computed tomography showing microscopic pore structures of coal.

2.3. Gas-Sealing Device. Before the testing, it is necessary to keep the sample under a constant gas pressure for 24 hours to ensure that the specimen is in the state of saturated adsorption gas. So, the mechanical experiment for testing gas-containing coal is difficult and strongly dependent on the gas sealing of the equipment. In order to achieve the gas tightness of the gas-sealing device, an O-type sealing ring is inserted between the glass window and gas-sealing device and ring cover plate and fixed with screws which are uniformly distributed on the cover plate, as shown in Figure 3. During the stress loading process, the pressure bar needs to slide down continuously, so the dynamic sealing element consisting of an O-type sealing ring and two YX-type sealing rings is adopted between the pressure bar and the gas-sealing device, as shown in Figure 2(a). In this study, the gas pressure sensor is used to measure the gas pressure inside the gas-sealing device to ensure the desired steady gas condition at room temperature for 24 hours before conducting the test. The gas tightness under different gas pressures is examined. As shown in Figure 4, the gas pressure decreases at the start along with the sealing time, which is due to the methane gas partially absorbed by the pore surface. After about five hours, the gas pressure reaches a stable value (i.e., 0.5 MPa, 1.0 MPa, and 1.5 MPa, respectively), which indicates that the gas-sealing device can provide a good gas sealing for tests.

2.4. Experimental Methods. UC, BD, and NCSB loading test are widely performed to measure uniaxial compressive strength, tensile strength, and fracture toughness, respectively [23, 24]. Three groups of specimens are prepared. The shapes and dimensions of the three testing methods of gas-containing coal specimens are shown in Figure 5. The detailed testing methods of gas-containing coal are presented as follows.

The UC tested prism specimens are 50 mm in height (H), 25 mm in width (W), and 25 mm in thickness (T). The BD-tested cylindrical specimens are 50 mm in diameter (D) and in thickness (T). The NSCB-tested specimens are 25 mm in radius (R), 5 mm in crack length (a), 20 mm in thickness (B), and 30 mm in span (2S). In the processing of NSCB specimens, semicircular specimens are cut along the diameter from rock core using a rotary diamond-impregnated saw with a thickness of 0.3 mm. Notch is machined from the disc center perpendicular to the diametrical direction using the diamond-impregnated saw. The crack tip of the notch is sharpened using a diamond wire saw with a thickness of 0.1 mm. The specimens for the UC, BD, and NSCB tests are prepared from the same block of raw coal. The original undisturbed coal is drilled perpendicular to a bedding plane to reduce the influence of bedding face on specimen strength. In this study, specimens without adsorbed gas are used for the control tests, and at least five samples are prepared to determine the mechanical parameters of the raw coal of each group. Five replicas are selected for each condition and with different gas pressures (i.e., 0.5, 1.0, and 1.5 MPa) controlled by the gas-sealing device at room temperature for 24 h.

The uniaxial compressive strength (σ_{uc}), tensile strength (σ_t), and fracture toughness (K_{IC}) [24] of coal rock samples of different gas pressures are calculated by using equations (1), (2), and (3), respectively.

$$\sigma_{uc} = \frac{F}{WT}, \tag{1}$$

$$\sigma_t = \frac{2F}{\pi DT}, \tag{2}$$

$$K_{IC} = Y_I\left(\frac{S}{R}\right)\frac{F\sqrt{\pi a}}{2RT}, \tag{3}$$

where F is the failure load, and $Y_I(S/R)$ is the fracture geometry factor of the sample type I crack.

In this study, $S/R = 15/25 = 0.6$, $a/R = 0.24$, and the fracture geometry factor of sample type I crack can be calculated by using the following equation [25]:

$$Y_I\left(\frac{S}{R}\right) = 3.286 - 0.432\left(\frac{a}{R}\right) + 0.039\exp\left[7.282\left(\frac{a}{R}\right)\right]. \tag{4}$$

3. Experimental Results

3.1. Fracture Modes of Gas-Containing Coal. Fracture modes are important characteristics to represent failure mechanism. The results of previous experiments show that shear failure is the main form of sample failure in UC test, and tensile failure is the main form in BD and NCSB loading test. Figure 6 shows the macroscopic fracture modes of the coal specimens for the UC, BD, and NSCB tests under different gas pressures. For the UC test result with no gas conditions, the "V" cone form of the failure surface is retained at the upper and lower ends of blocks, which mainly shows shear fracture; the failure morphology is similar to that of hard rock testing [26] (as depicted in Figure 6(a)). However, the obvious lamellar fracture damage is retained within specimens (position of lamellar fracture showed by red arrows) with a gas pressure of 1.5 MPa, which mainly shows tensional fracture (as presented in Figure 6(b)). For the BD and NSCB testing, the tensional fracture is the major fracture mode under different gas pressure conditions. The form of crack propagation in the uniaxial compressive test is significantly changed by the gas

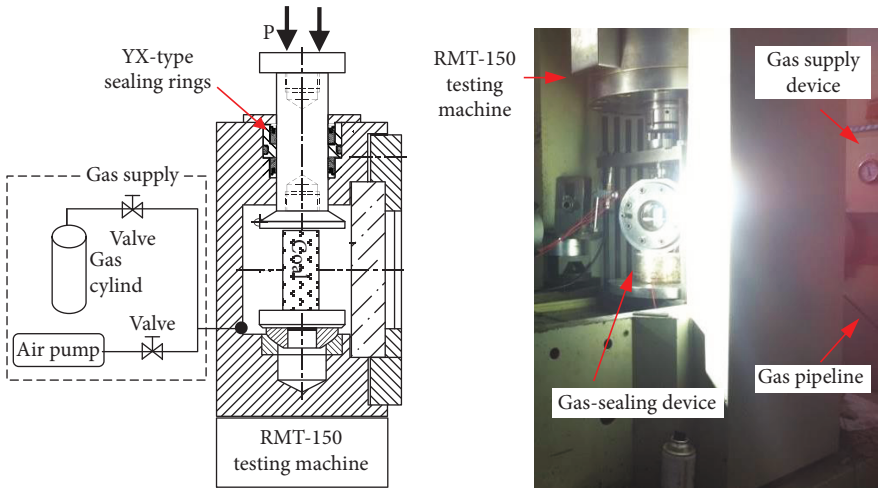

Figure 2: Experimental system for gas-containing coal schematics (a) and device (b).

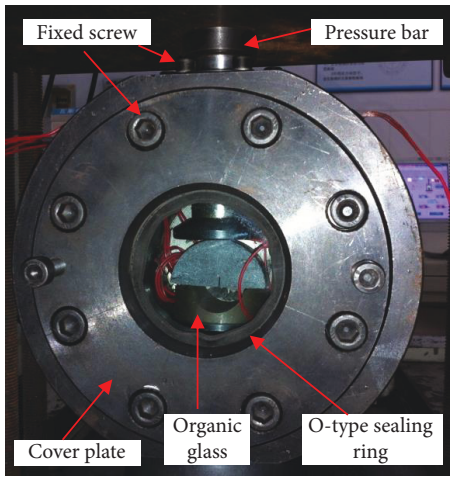

Figure 3: Gas-sealing device.

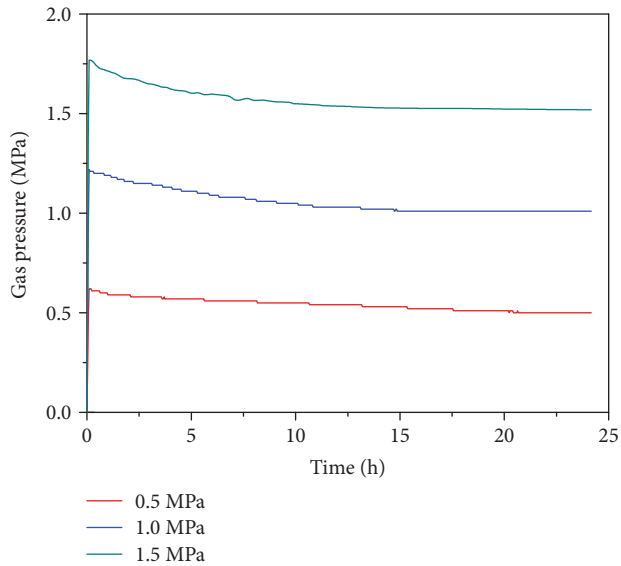

Figure 4: Gas pressure time histories before test.

state on the coal specimens. With increasing gas pressure, the mode of crack propagation is changed from traditional shear failure to tensile failure. In the state of high gas pressure, the tensile failure is obvious in uniaxial compressive, BD, and NCSB loading test.

In the field of underground coal mining, the mining-induced stress of coal seam in the front of the working face is increased; the coal seam is under obvious compressive stress, and the gas pressure also increases [1]. The results of this study show that the mode of crack propagation of gas-containing coal gradually changes to tensile failure as gas pressure increases. The mechanical parameters of tensile failure are smaller than those of other forms of failure, and the tensile failure is likely to occur under the same external conditions [27]. Therefore, in the analysis of the safety stability of gas-containing coal based on crack propagation, mechanical parameters, such as fracture toughness or tensile strength, which can directly reflect the tensile properties of materials, should be emphasized.

3.2. Strength Characteristics of Gas-Containing Coal. The mechanical parameters, such as uniaxial compressive strength (σ_{uc}), tensile strength (σ_t), and fracture toughness (K_{IC}), of the specimens under the UC, BD, and NSCB loading test are calculated using equations (1), (2), and (3), respectively. All the tested specimens at various initial gas pressures in this study are summarized in Table 1. The initial gas pressure affects the mechanical parameters of the coal specimens. As the gas pressure increases from no gas pressure to 1.5 MPa, the average σ_{uc} decreases from 23.54 to 13.75, the average σ_t decreases from 1.99 to 0.60, and K_{IC} decreases from 0.44 to 0.17. The gas attenuation coefficient is defined as the ratio between the change value of mechanical parameters under different gas pressures and the value of mechanical parameters without gas to compare the variation degree of mechanical parameters as affected by gas. In the

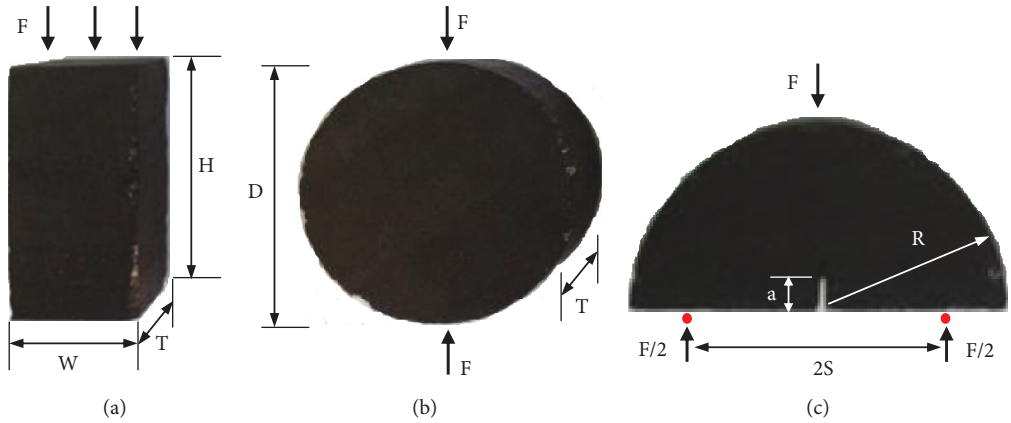

Figure 5: Optical deformation measurement device (a) UC testing, (b) BD testing, and (c) NSCB testing.

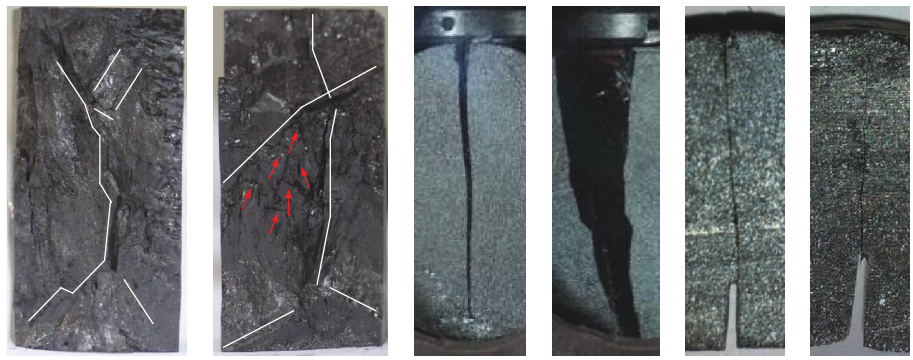

Figure 6: Failure patterns of gas-containing coal changing with gas pressures (a) UC test with no gas, (b) UC test with 1.5 MPa gas pressure, (c) BD test with no gas, (d) BD test with 1.5 MPa gas pressure, (e) NSCB test with no gas, and (f) NSCB test with 1.5 MPa gas pressure.

studies by Wang et al. [28–31], the mechanical properties of coal were investigated and the effect of contained free water on the properties was discussed. The material strength and fracture resistance of the coal increase with the increasing water content, which is different from the performance of the gas-containing coal with the increasing gas pressure. It should be noted that the water viscosity affects the evolution of microcracks and micropores while the gas viscosity has a little effect on the material properties. It should be also noted that the damage on the specimen during loading causes gas desorption which leads to the increase of gas pressure inside the gas-containing coal. Therefore, the gas-containing coal experiences more severe damage under the condition of high gas pressure under the external load. The attenuation law of the mechanical properties of gas-containing coal under different gas pressures is shown in Figure 7.

Figure 7 indicates that with increasing gas pressure, the attenuation coefficient of mechanical properties under UC, BD, and NSCB loading test with different gas pressures can be represented by linear function relationship, and the attenuation coefficient of the different loading tests of gas-containing coal is obviously different. The attenuation coefficient of uniaxial compressive strength is approximately 41.59% with increasing gas pressure from no gas to 1.5 MPa, which is significantly smaller than that of tensile strength (69.85%) and fracture toughness (61.19%). The influence of gas state on the attenuation of tensile failure is accordingly obvious. As influenced by deep mining of high-gas coal seam, the tensile stress in the area near the working face is produced by the mining unloading process under high stress [32]. The gas states significantly reduce the tensile strength. Therefore, the tensile failure of coal body caused by strong unloading during mining should be avoided.

3.3. Correlation Analysis of the Fracture Toughness and Strength Parameters of Gas Coal under Different Gas Pressures. Crack propagation is a key factor in the fracture of rock-like materials, and the linear elastic fracture mechanics is widely used for fracture analysis, in which fracture toughness is an important parameter [33]. In this study, three experimental schemes are adopted to measure the mechanical parameters (i.e., σ_{uc}, σ_t, and K_{IC}). Some problems occur with the measurement of fracture toughness by NSCB testing, such as difficult to process specimens with prefabricated cracks and to capture the fracture toughness critical point caused by early failure. Therefore, for field engineering, a simple and effective method is needed to measure fracture

Table 1: Mean values of uniaxial compressive strength (σ_{uc}), tensile strength (σ_t), and fracture toughness (K_{IC}) of coal under different gas pressures.

Specimen	σ_{uc} (MPa)	Average σ_{uc}	$\Delta\ \sigma_{uc}$ (%)	σ_t (MPa)	Average σ_t	$\Delta\ \sigma_t$ (%)	K_{IC} (MPa·m$^{1/2}$)	Average K_{IC}	$\Delta\ K_{IC}$ (%)
No gas									
1	22.79			2.13			0.45		
2	24.66			2.25			0.45		
3	20.51	23.54	—	1.06	1.99	—	0.43	0.44	—
4	27.85			2.77			0.46		
5	21.88			1.76			0.44		
0.5 MPa									
1	19.73			1.62			0.36		
2	23.2			2.44			0.39		
3	20.68	19.7	16.31	1.94	1.64	17.68	0.37	0.34	22.56
4	18.9			1.17			0.30		
5	15.96			1.04			0.30		
1.0 MPa									
1	16.12			1.12			0.22		
2	12.61			0.75			0.22		
3	13.4	15.71	33.26	1.05	1.24	38.00	0.22	0.24	46.56
4	18.81			1.98			0.30		
5	17.64			1.29			0.23		
1.5 MPa									
1	14.04			0.54			0.19		
2	17.8			1.01			0.23		
3	12.26	13.75	41.59	0.43	0.60	69.85	0.12	0.17	61.19
4	9.03			0.33			0.11		
5	15.62			0.70			0.21		

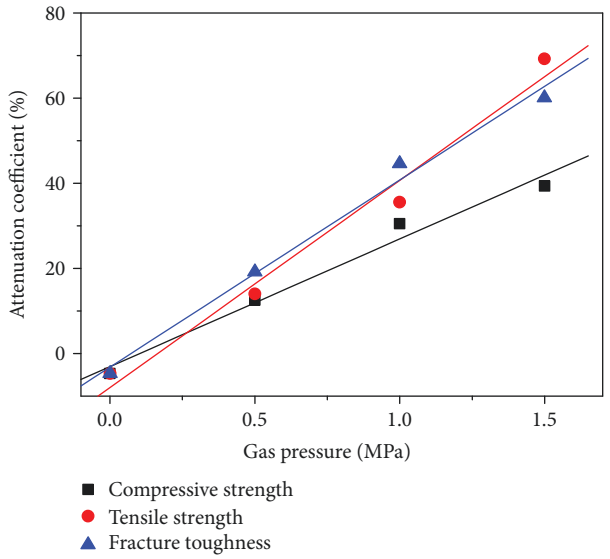

Figure 7: Attenuation coefficient of mechanical properties of gas-containing coal under different gas pressures.

toughness. Previous studies have shown that the fracture toughness of rock-like materials is related to tensile strength and compressive strength [34, 35]; one of the dominated reasons for the destruction of rock materials is the expansion of microcracks, and the main reason for the expansion of the microcracks is tensile stress rather than compressive and shear stresses.

The relationship among the fracture toughness, compressive strength, and tensile strength of gas-containing coal under different gas pressure conditions is obtained in this study through the statistics of the experimental data, as shown in Figures 8 and 9. Fracture toughness has a good linear relationship with the tensile strength and compressive strength of the gas-containing coal with different initial gas pressures. The linear relationship is shown in Table 2. Fracture toughness is positively correlated with compressive strength and tensile strength, and the positive correlation coefficient increases with the increase in gas pressure. The linear relationship between fracture toughness and tensile strength is better than that between fracture toughness and compressive strength. As the gas pressure increases from no gas to 1.5 MPa, the coefficients of determination of the linear relationship between fracture toughness and uniaxial compressive strength are 0.84, 0.78, 0.56, and 0.89, and the coefficients of determination of the linear relationship between

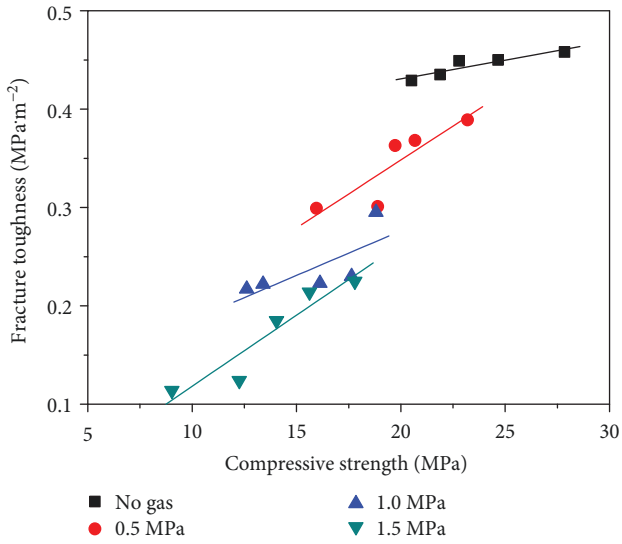

Figure 8: Relationship of fracture toughness against compressive strength under different gas pressures.

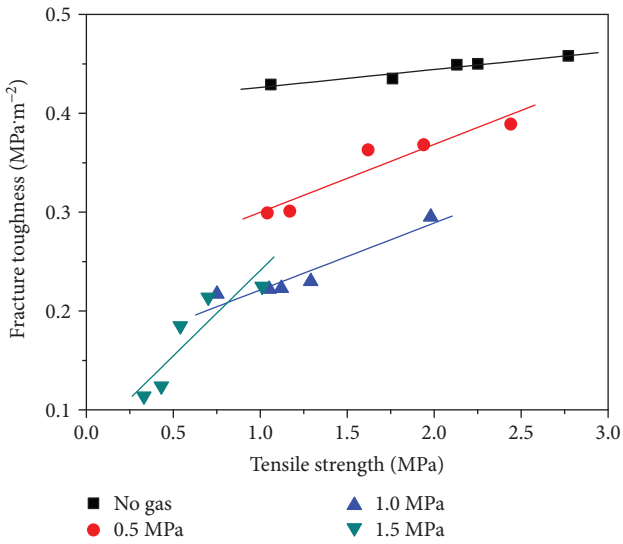

Figure 9: Relationship of fracture toughness against tensile strength under different gas pressures.

Table 2: Fitting function relationships.

Relationship	Gas pressure	Fitting function	R^2
σ_{uc}-K_{IC}	No gas	$K_{IC} = 0.004\sigma_{uc} + 0.354$	0.84
	0.5 MPa	$K_{IC} = 0.014\sigma_{uc} + 0.072$	0.78
	1.0 MPa	$K_{IC} = 0.009\sigma_{uc} + 0.095$	0.56
	1.5 MPa	$K_{IC} = 0.014\sigma_{uc} - 0.026$	0.89
σ_t-K_{IC}	No gas	$K_{IC} = 0.018\sigma_t + 0.408$	0.94
	0.5 MPa	$K_{IC} = 0.069\sigma_t + 0.231$	0.9
	1.0 MPa	$K_{IC} = 0.068\sigma_t + 0.154$	0.91
	1.5 MPa	$K_{IC} = 0.173\sigma_t + 0.068$	0.82

fracture toughness and uniaxial compressive strength are 0.94, 0.90, 0.91, and 0.82. With the increase in gas pressure from 0 MPa to 1.5 MPa, in case of $\sigma_t = 0$, the calculated value of K_{IC} using the fitting formula is reduced from 0.408 to 0.068. The linear relation between the fracture toughness and tensile strength of gas-containing coal is close to the theoretical value with increasing gas pressure. Therefore, the fracture toughness of the gas-containing coal can be accurately predicted by BD testing, which will simplify the test of fracture toughness.

4. Discussion

4.1. Basic Model of the Action of Gas in Coal. Coal is a complex porous medium composed of solid skeleton and pores, and its pores are gas storage sites and flow channels. The gas adsorption on the surface of coal pores without mining-induced stress leads to a relative equilibrium under the joint action of in-situ stress and free gas pressure. With the influence of coal mining, the pores are deformed by the changes in mining-induced stress, and the partial adsorbed gas is changed into free forms. For low-permeability coal, the free gas in the pores cannot flow well, which causes the gas pressure in the pores to increase. Therefore, the stress balance of the surrounding area of the pores is changed. The geometrical features of pores (i.e., occurring elements, density, gap width, and connection degree) in real coal are complex. Two assumptions are established to analyze the crack propagation characteristics of gas-containing coal under gas desorption and external loads. First, the permeability of coal pores is low, and the pore surface is flat. Second, the effective gas desorption rate α is defined, the amount of gas desorption has a positive correlation with the initial gas pressure, and the correlation coefficient is α. The stress models of gas-containing coal are shown in Figure 10.

4.2. Effect of Gas Pressure on the Stress Intensity Factors. The test results and theoretical calculations show that cracking angle is perpendicular to the maximum tensile stress, as mode I crack propagation. The cracking angle is influenced by stratum stress σ_1. The increment in the gas pressure in pores ($\triangle p$), the effective normal stress (σ_N), the lateral compressive stress (σ_T), and the shear stress (τ) are derived on the crack plane as follows:

$$\left.\begin{aligned} \tau &= \frac{1}{2}\sigma_1 \sin 2\beta, \\ \sigma_N &= \frac{1}{2}(\sigma_1 + \sigma_1 \cos 2\beta) - \Delta p, \\ \sigma_T &= \frac{1}{2}(\sigma_1 - \sigma_1 \cos 2\beta) - \Delta p, \end{aligned}\right\} \quad (5)$$

where β is the crack inclination angle.

A power correlation was investigated between the quantity of initial gas pressure and the amount of desorption gas by Wei et al. [36], who measured the gas desorption index of outburst coal seams from the Gaocheng mine in China. The gas pressure increment ($\triangle p$) is calculated by the initial

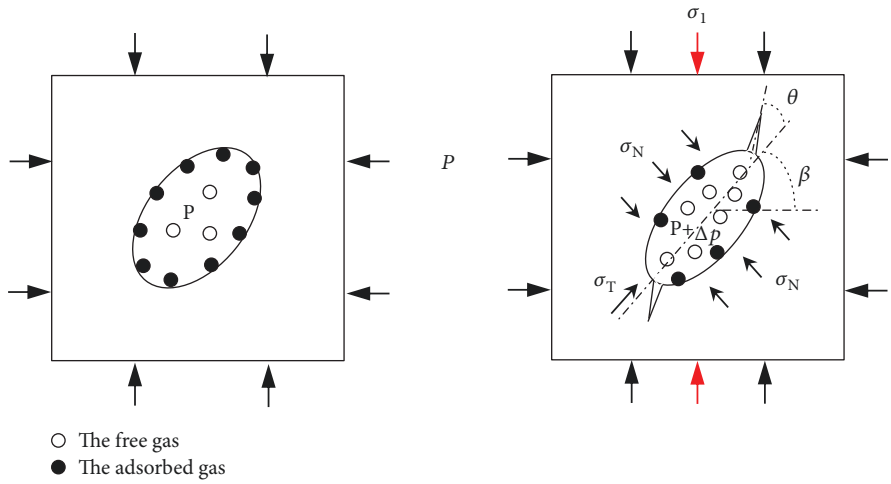

Figure 10: Schematic diagram for the pores deformation of gas-containing coal (a) Initial state, (b) Static loading.

gas pressure and the desorption rate according to the following ideal gas equation:

$$\Delta p = \alpha A P^B, \tag{6}$$

where A and B are constant.

A new relationship of the stress intensity factors of modes I crack tip (K_I) and II crack tip (K_{II}) is proposed by the theory of fracture mechanics as follows:

$$\begin{aligned} K_I &= K_{I(N)} + K_{I(T)} = -\sigma_N\sqrt{\pi a} + \sigma_T\sqrt{\frac{\rho}{a}}\sqrt{\pi a} \\ &= -\sqrt{\pi a}\left[\frac{1}{2}(\sigma_1 + \sigma_1\cos 2\beta) - \alpha A P^B\right] \\ &\quad + \sqrt{\pi a}\left[\frac{1}{2}(\sigma_1 - \sigma_1\cos 2\beta) - \alpha A P^B\right]\sqrt{\frac{\rho}{a}}, \end{aligned} \tag{7}$$

$$K_{II} = -\tau\sqrt{\pi a} = -\frac{1}{2}\sqrt{\pi a}\sigma_1 \sin 2\beta, \tag{8}$$

where $K_{I(N)}$ and $K_{I(T)}$ are the stress intensity factors induced by the effective normal stress (σ_N) and lateral compressive stress (σ_T), a is the crack length, and ρ is the radius of the curvature of the crack tip.

The proposed relationship shows that K_I is directly proportional to P and α, but K_{II} has no correlation with P and α. Figure 11 shows the sensitivity of P and α to a multiplication factor of K_I under the same external loading. As gas pressure increases, the stress intensity factors increase at the same gas desorption rate. The figure indicates that the increment rate of K_I is high with increasing gas desorption rate. Under the same external loading and gas pressure of 1.5 MPa, the stress intensity factor of crack tip at 100% gas desorption rate is approximately 10 times higher than that at 10% gas desorption rate.

4.3. Effect of Gas Pressure on Cracking Angle. A wing cracking from the tip of initial crack in direction θ, wherein the transformed mode I stress intensity factor produced by hoop

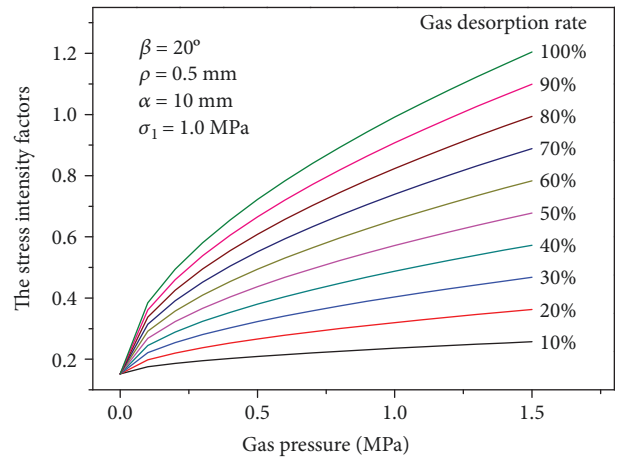

Figure 11: Sensitivity of incident gas desorption rate and gas pressure of gas-containing coal to K_I prediction.

stress is maximum and greater than the fracture toughness K_{IC} of rock material, is the critical stress intensity factor in mode I. The transformed stress intensity factor $K_I(\theta)$ given by [37] is expressed as

$$K_I(\theta) = K_I\cos^3\frac{\theta}{2} - \frac{3}{2}K_{II}\sin\theta\cos\frac{\theta}{2}. \tag{9}$$

The crack extension criteria are defined as follows:

$$\begin{aligned} \frac{\partial K_I(\theta)}{\partial\theta} &= 0, \\ \frac{\partial^2 K_I(\theta)}{\partial\theta^2} &< 0. \end{aligned} \tag{10}$$

A gas desorption rate of 10% is taken for example, and the influence law of initial crack angle in gas retention is obtained according to equations (7), (8), (9), and (10), as shown in Figure 12. Crack initiation angle exerts a minimal influence on the initial cracking angle, but as the gas pressure

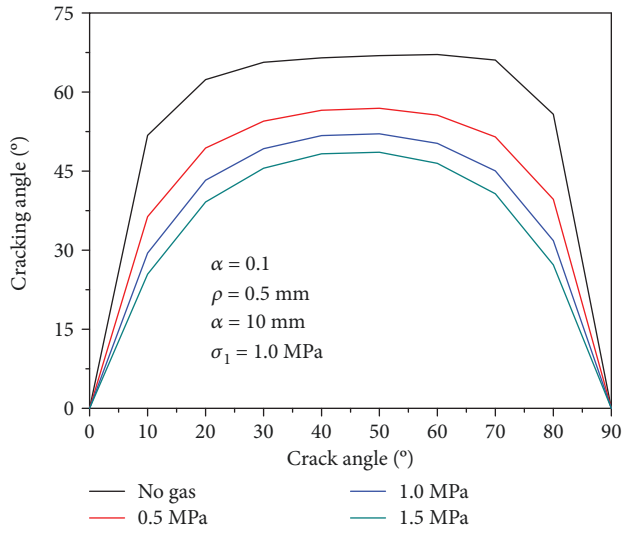

Figure 12: Relationship of cracking angle against cracking angle under different gas pressures.

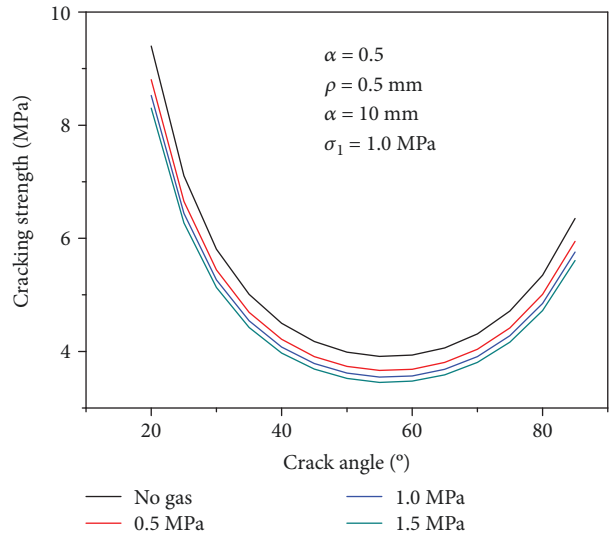

Figure 13: Relationship of cracking strength against crack angle under different gas pressures.

increases, it decreases. With no gas state, the initial cracking angle is approximately 70°. This phenomenon is consistent with the results reported by Li et al. [38], who measured the cracking angle of rock under seepage pressure and far-field stress. The initial angles of crack of 40° and 50° are taken for example. As the gas pressure increases from 0 MPa to 1.5 MPa, the cracking angle reduces from 66.5° and 66.9° to 48.3°and 48.6°, respectively. The cracking angle decreases nearly by 30%. The maximum circumferential direction of the crack tip can be changed by the gas pressure during crack propagation. With increasing gas pressure, the extension angle of the wing crack becomes close to the crack inclination angle, which leads to the failure mode as tensional fracture that is consistent with the experimental results in this study.

4.4. Effect of Gas Pressure on Cracking Strength. The compression–shear fracture criterion with compression–shear coefficient λ_{12} was introduced on the basis of the theory of Mohr–Coulomb strength by Zhou [39], as the following equation:

$$\lambda_{12}\sum K_{\mathrm{I}}+\sum K_{\mathrm{II}} = K_{\mathrm{IIC}}, \tag{11}$$

where K_{IIC} is the fracture toughness of type II crack, and the K_{IIC} of sample can be calculated by K_{IC} [40] as $K_{\mathrm{IIC}} = 0.866\,K_{\mathrm{IC}}$.

Equations (7) and (8) are substituted into Equation (11), and the crack compression–shear fracture intensity of coal under gas desorption pressure can be derived as follows:

$$\begin{aligned}
\sigma_1 &= \frac{2K_{\mathrm{IIC}}/\sqrt{\pi a} + A\sigma_3 + 2\alpha A P^B \lambda_{12}(\sqrt{\rho/a}-1)}{B},\\
A &= \sin 2\beta + \lambda_{12}(1-\cos 2\beta) - \sqrt{\frac{\rho}{a}}(1+\cos 2\beta),\\
B &= \sin 2\beta + \lambda_{12}\left[\sqrt{\frac{\rho}{a}}(1-\cos 2\beta) - (1+\cos 2\beta)\right].
\end{aligned} \tag{12}$$

The initial cracking intensity of crack under different gas pressures can be calculated according to the experimental results in this study, as shown in Figure 13. With the increase in gas pressure, the cracking strength decreases. The results of the theoretical analysis of stress intensity factors, cracking angle, and cracking strength show that with the increase in gas pressure, the crack tip stress intensity factor increases, whereas the cracking angle and strength decrease. These results indicate the significant influence of the initial gas pressure on the crack propagation of coal specimen, and tensional fracture is likely to happen. A gas pressure of 1 MPa and an external load of 1.5 MPa are taken for example. The normal effective stress (*ES*) and the cracking strength (*CS*) are calculated in the desorption rates of 0, 20%, 40%, and 60%, as shown in Figure 14. At a gas desorption rate of 0 (as no gas state) and an external load of 1.5 MPa, the normal effective stress of the crack tip is obviously lower than the cracking strength; consequently, cracks cannot expand. With increasing gas desorption rate, the crack tip effective stress is increased, but the cracking stress is decreased. At a gas desorption rate of 0.6, some crack's effective stress is greater than the cracking strength, in which the crack angle is between 30° and 80°. Thus, under the same external load (as 1.5 MPa), the possibility of crack expansion is increased as the gas desorption rate increases.

Figures 13 and 14 show that the initial gas pressure and gas desorption rate affect the effective stress and cracking strength of the gas-containing coal specimens. As the initial gas pressure or the gas desorption rate increases, the crack stress intensity factors and effective stress of gas-containing coal increase, whereas the cracking strength decreases. In the process of coal mining of deep high-gas coal mines, the cracks of gas-containing coal propagate under small external loads (as mining-induced stress). Instability and failure of coal then occur, and the failure may result in serious consequences, such as coal and gas outburst accidents. Previous studies have indicated that in the high gas-containing and

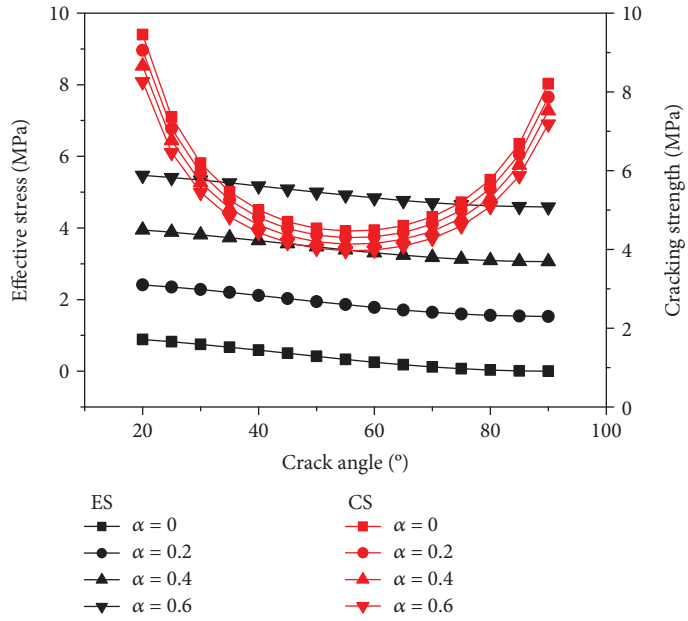

Figure 14: Relationship of effective stress against crack angle under different gas desorption rate.

low-permeability coal seams of deep coal mines, an increase in external load will induce the increase in gas desorption rate and gas pressure. Therefore, in the mining process of deep low-permeability coal seams, not only the gas pressure must be ensured to meet the requirements of safe mining, but also the influence of the disturbance of mining-induced stress on the desorption degree of the adsorption gas must be considered. Coal and gas outburst accidents can be avoided by reducing the disturbance of mining-induced stress and accumulation of free gas and ensuring the safety of coal seam mining.

5. Conclusions

The mechanical properties (i.e., uniaxial compressive strength, tensile strength, and fracture toughness) of gas-containing coal with four levels of initial gas pressure (i.e., 0.0, 0.5, 1.0, and 1.5 MPa) are investigated in this study by using a newly developed gas-sealing device and an RMT-150 rock mechanics testing machine. The fracture modes and the correlation among fracture toughness, compressive strength, and tensile strength are examined. The experimental results are verified by the theoretical analysis of crack initiation characteristics based on fracture mechanics.

Theoretical and experimental analyses show that the uniaxial compressive strength, tensile strength, and fracture toughness of gas-containing coal decrease as the initial gas pressure increases. The fracture mode of gas-containing coal is mainly the tensile failure. An obvious linear correlation exists between tensile strength and fracture toughness under a high initial gas pressure. This study is meaningful to the design and construction of high-gas and low-permeability coal seams for deep mining. When the working face is at a great depth and a high gas pressure, coal stability might be vulnerable to high mining-induced stress.

In the further study, special attention should be devoted to the accumulation of mining-induced stress and free gas in the mining of deep mines in high-gas coal seams to prevent induced dynamic disaster accidents under coupled mining-induced stress and gas pressure. The mode of reasonable reduction of mining-induced stress is necessary to be further researched, given that mining-induced stress is unavoidable in coal mining. Further test analysis of the effects of gas state and mining-induced stress on the permeability of gas-containing coal is suggested to be conducted to reduce the accumulation of free gas by improving the permeability of coal seams.

Data Availability

The data used to support the findings of this study are included within the article.

Conflicts of Interest

The authors declare that there are no conflicts of interest regarding the publication of this article.

Acknowledgments

This work was supported by the National Natural Science Foundation of China (71874006, 51774009), Anhui Provincial Natural Science Foundation (1808085ME159, 1808085QE149, and 1808085ME134), Science and Technology Planning Project of Anhui Province (1604a0802107), and Program for Innovative Research Team in the University of Anhui Province (prevention and control of coal rock dynamic disasters in deep coal mine).

References

[1] G. Xie, Z. Yin, Z. Hu, J. Hou, and H. Ma, "Disaster-causing mechanical mechanism of coal mining dilatancy of gassy seam in deep mine," *Journal of China Coal Society*, vol. 40, no. 1, pp. 24–29, 2015.

[2] H. Alehossein and B. A. Poulsen, "Stress analysis of longwall top coal caving," *International Journal of Rock Mechanics and Mining Sciences*, vol. 47, no. 1, pp. 30–41, 2010.

[3] S. Xue, L. Yuan, J. Wang, Y. Wang, and J. Xie, "A coupled DEM and LBM model for simulation of outbursts of coal and gas," *International Journal of Coal Science & Technology*, vol. 2, no. 1, pp. 22–29, 2015.

[4] G. Jing and Q. Zhang, "Study on the role of gas in the coal and gas outburst," *Journal of China Coal Society*, vol. 30, no. 2, pp. 169–171, 2005.

[5] Z. Wang, G. Yin, Q. Hu, and H. Jin, "Inducing and transforming conditions from rockburst to coal-gas outburst in a high gassy coal seam," *Journal of Mining and Safety Engineering*, vol. 27, no. 4, pp. 572–580, 2010.

[6] C. W. Li, B. J. Jie, G. L. Cao, T. T. Wang, and X. Y. Wang, "The energy evaluation model of coal and gas outburst intensity," *Journal of China Coal Society*, vol. 37, no. 9, pp. 1547–1552, 2012.

[7] G. Wang, M. Wu, H. Wang, Q. Huang, and Y. Zhong, "Sensitivity analysis of factors affecting coal and gas outburst based on a energy equilibrium model," *Chinese Journal of Rock Mechanics and Engineering*, vol. 34, no. 2, pp. 238–248, 2015.

[8] J. Litwiniszyn, "Rarefaction shock waves in porous media that accumulate CO_2, CH_4, N_2," *Shock Waves*, vol. 3, no. 3, pp. 223–232, 1994.

[9] A. D. Alexeev, V. N. Revva, N. A. Alyshev, and D. M. Zhitlyonok, "True triaxial loading apparatus and Its application to coal outburst prediction," *International Journal of Coal Geology*, vol. 58, no. 4, pp. 245–250, 2004.

[10] G. Yin, H. Qin, G. Huang, Y. Lv, and Z. Dai, "Acoustic emission from gas-filled coal under triaxial compression," *International Journal of Mining Science and Technology*, vol. 22, no. 6, pp. 775–778, 2012.

[11] D. Yang, Y. Chen, J. Tang et al., "Experimental research into the relationship between initial gas release and coal-gas outbursts," *Journal of Natural Gas Science and Engineering*, vol. 50, pp. 157–165, 2018.

[12] G. Xie, Z. Yin, L. Wang, Z. Hu, and C. Zhu, "Effects of gas pressure on the failure characteristics of coal," *Rock Mechanics and Rock Engineering*, vol. 50, no. 7, pp. 1711–1723, 2017.

[13] P. G. Ranjith, D. Jasinge, S. K. Choi, M. Mehic, and B. Shannon, "The effect of CO_2 saturation on mechanical properties of Australian black coal using acoustic emission," *Fuel*, vol. 89, no. 8, pp. 2110–2117, 2010.

[14] L. Meng, H. W. Wang, X. H. Li, and Y. X. Zhao, "Investigation on acoustic emission characteristics in failure process of coal absorbed methane," *Journal of China Coal Society*, vol. 39, no. 2, pp. 377–383, 2014.

[15] J. Xu, Y. Liang, D. Liu, L. Cheng, L. Wang, and X. Song, "Experimental study of crack's meso-characteristics of raw coal subjected to direct shear load under different gas pressures," *Chinese Journal of Rock Mechanics and Engineering*, vol. 31, no. 12, pp. 2431–2437, 2012.

[16] Z. Yin, G. Xie, Z. Hu, and C. Zhu, "Investigation on fracture mechanism of coal rock on three-point bending tests under different gas pressures," *Journal of China Coal Society*, vol. 41, no. 2, pp. 424–431, 2016.

[17] S. Harpalani, B. K. Prusty, and P. Dutta, "Methane/CO_2 sorption modeling for coalbed methane production and CO_2 sequestration," *Energy & Fuels*, vol. 20, no. 4, pp. 1591–1599, 2006.

[18] C. R. Clarkson, Z. Pan, I. D. Palmer, and S. Harpalani, "Predicting sorption-induced strain and permeability increase with depletion for coalbed-methane reservoirs," *SPE Journal*, vol. 15, no. 1, pp. 152–159, 2010.

[19] R. Feng, S. Harpalani, and R. Pandey, "Evaluation of various pulse-decay laboratory permeability measurement techniques for highly stressed coals," *Rock Mechanics and Rock Engineering*, vol. 50, no. 2, pp. 297–308, 2017.

[20] M. C. He, C. G. Wang, J. L. Feng, D. J. Li, and G. Y. Zhang, "Experimental investigations on gas desorption and transport in stressed coal under isothermal conditions," *International Journal of Coal Geology*, vol. 83, no. 4, pp. 377–386, 2010.

[21] J. Fan, R. Feng, J. Wang, and Y. Wang, "Laboratory investigation of coal deformation behavior and its influence on permeability evolution during methane displacement by CO_2," *Rock Mechanics and Rock Engineering*, vol. 50, no. 7, pp. 1725–1737, 2017.

[22] Y. Li, Y. F. Chen, and C. B. Zhou, "Effective stress principle for partially saturated rock fractures," *Rock Mechanics and Rock Engineering*, vol. 49, no. 3, pp. 1091–1096, 2016.

[23] Q. B. Zhang and J. Zhao, "Determination of mechanical properties and full-field strain measurements of rock material under dynamic loads," *International Journal of Rock Mechanics and Mining Sciences*, vol. 60, pp. 423–439, 2013.

[24] F. Q. Gong, S. Luo, and J. Y. Yan, "Energy storage and dissipation evolution process and characteristics of marble in three tension-type failure tests," *Rock Mechanics and Rock Engineering*, vol. 51, no. 11, pp. 3613–3624, 2018.

[25] Y. L. Liu, D. A. Cendón, P. W. Chen, and K. D. Dai, "Fracture of PBX notched specimens: experimental research and numerical prediction," *Theoretical and Applied Fracture Mechanics*, vol. 90, pp. 268–275, 2017.

[26] F. Q. Gong, Y. Luo, X. B. Li, X. F. Si, and M. Tao, "Experimental simulation investigation on rockburst induced by spalling failure in deep circular tunnels," *Tunnelling and Underground Space Technology*, vol. 81, pp. 413–427, 2018.

[27] D. Li, C. C. Li, and X. Li, "Influence of sample height-to-width ratios on failure mode for rectangular prism samples of hard rock loaded in uniaxial compression," *Rock Mechanics and Rock Engineering*, vol. 44, no. 3, pp. 253–267, 2011.

[28] W. Wang, H. Wang, D. Li, H. Li, and Z. Liu, "Strength and failure characteristics of natural and water-saturated coal specimens under static and dynamic loads," *Shock and Vibration*, vol. 2018, Article ID 3526121, 15 pages, 2018.

[29] W. Wang, H. Li, and H. Gu, "Experimental study of strength characteristics of water-saturated coal specimens under 3D coupled static-dynamic loadings," *Chinese Journal of Rock Mechanics and Engineering*, vol. 36, no. 10, pp. 2406–2414, 2018.

[30] W. Wang, H. Li, R. Yuan, H. Gu, C. Wang, and H. Li, "Micromechanics analysis and mechanical characteristics of water-saturated coal samples under coupled static-dynamic loads," *Journal of China Coal Society*, vol. 41, no. 3, pp. 611–617, 2016.

[31] W. Wang, H. Li, H. Gu, and C. Wang, "Feature analysis of energy dissipation of water-saturated coal samples under coupled static-dynamic loads," *Chinese Journal of Rock Mechanics and Engineering*, vol. 34, no. S2, pp. 3965–3971, 2015.

[32] M. Tao, X. Li, and D. Li, "Rock failure induced by dynamic unloading under 3D stress state," *Theoretical and Applied Fracture Mechanics*, vol. 65, pp. 47–54, 2013.

[33] M. F. Kanninen and C. L. Popelar, *Advanced Fracture Mechanics*, Oxford University Press, 1985.

[34] Z. X. Zhang, "An empirical relation between mode I fracture toughness and the tensile strength of rock," *International Journal of Rock Mechanics and Mining Sciences*, vol. 39, no. 3, pp. 401–406, 2002.

[35] J.-J. Wang, J.-G. Zhu, C. F. Chiu, and H. Zhang, "Experimental study on fracture toughness and tensile strength of a clay," *Engineering Geology*, vol. 94, no. 1-2, pp. 65–75, 2007.

[36] F. Wei, G. Shi, and T. Zhang, "Study on coal and gas outburst prediction indexes base on gas expansion energy," *Journal of China Coal Society*, vol. 35, no. S, pp. 95–99, 2010.

[37] F. Erdogan and G. C. Sih, "On the crack extension in plates under plane loading and transverse shear," *Journal of Basic Engineering*, vol. 85, no. 4, pp. 519–525, 1963.

[38] X. Li, X. He, and H. Chen, "Crack initiation characteristics of opening-mode creck embedded in rock-like material under seepage pressure," *Chinese Journal of Rock Mechanics and Engineering*, vol. 31, no. 7, pp. 1317–1324, 2012.

[39] Q. Zhou, "Compress shear fracture criterion of rock and its application," *Geotechnical Engineering*, vol. 9, no. 5, pp. 33–37, 1987.

[40] J. Zhou, W. Xu, and C. Shi, "Investigation on compression-shearfracture criterion of rock based on failure criteria," *Chinese Journal of Rock Mechanics and Engineering*, vol. 26, no. 6, pp. 1194–1201, 2007.